Published in final edited form as:
Science. 2010 March 5; 327(5970): 1223–1228. doi:10.1126/science.1182228.

Sestrin as a feedback inhibitor of TOR that prevents age-related pathologies

Jun Hee Lee[1], **Andrei V. Budanov**[1], **Eek Joong Park**[1], **Ryan Birse**[2], **Teddy E. Kim**[3], **Guy A. Perkins**[4], **Karen Ocorr**[2], **Mark H. Ellisman**[4], **Rolf Bodmer**[2], **Ethan Bier**[3], and **Michael Karin**[1,†]

[1]Laboratory of Gene Regulation and Signal Transduction, Departments of Pharmacology and Pathology, School of Medicine, University of California San Diego, La Jolla, CA, USA

[2]Development and Aging Program, NASCR Center, Burnham Institute for Medical Research, La Jolla, CA, USA

[3]Section of Cell and Developmental Biology, University of California San Diego, La Jolla, CA, USA

[4]National Center for Microscopy and Imaging Research, and Department of Neurosciences, University of California San Diego, La Jolla, CA, USA

Abstract

Sestrins are conserved proteins that accumulate in cells exposed to stress and potentiate adenosine monophosphate-activated protein kinase (AMPK) and inhibit activation of target of rapamycin (TOR). We show that abundance of *Drosophila* Sestrin (dSesn) is increased upon chronic TOR activation through accumulation of reactive oxygen species (ROS) that cause activation of c-Jun N-terminal kinase (JNK) and transcription factor FoxO (Forkhead box O). Loss of dSesn resulted in age-associated pathologies including triglyceride accumulation, mitochondrial dysfunction, muscle degeneration and cardiac malfunction, which were prevented by pharmacological activation of AMPK or inhibition of TOR. Hence, dSesn appears to be a negative feedback regulator of TOR that integrates metabolic and stress inputs and prevents pathologies caused by chronic TOR activation, that may result from diminished autophagic clearance of damaged mitochondria, protein aggregates, or lipids.

TOR (target of rapamycin) is a key protein kinase that regulates cell growth and metabolism to maintain cellular and organismal homeostasis (1-3). Insulin (Ins) and insulin-like growth factors (IGF) are major TOR activators that operate through phosphoinositide 3-kinase (PI3K) and the protein kinase AKT (2). Conversely, adenosine monophosphate activated protein kinase (AMPK), which is activated upon energy depletion, caloric restriction (CR), or genotoxic damage, is a stress-responsive inhibitor of TOR activation (2,4). TOR stimulates cell growth and anabolism by increasing protein and lipid synthesis through p70 S6 kinase (S6K), eukaryotic translation initiation factor 4E-binding protein (4E-BP), and sterol response element binding protein (SREBP) (1-3,5) and by decreasing autophagic

[†]To whom correspondence should be addressed. karinoffice@ucsd.edu.

Supporting Online Material
www.sciencemag.org
Materials and Methods
Figs. S1 to S21
Movies S1 to S8
References

catabolism through phosphorylation-mediated inhibition of ATG1 protein kinase (1,6). Persistent TOR activation is associated with diverse pathologies such as cancer, diminished cardiac performance, and obesity-associated metabolic diseases (1). Conversely, inhibition of TOR prolongs life span and increases quality-of-life by reducing the incidence of age-related pathologies (1-3,7). The anti-aging effects of CR could be due to inhibition of TOR (8).

Sestrins (Sesns) are highly conserved proteins that accumulate in cells exposed to stress, lack obvious domain signatures, and have poorly defined physiological functions (9,10). Mammals express three Sesns, whereas *D. melanogaster* and *C. elegans* have single orthologues (fig. S1, A and B). In vitro, Sesns exhibit oxidoreductase activity and may function as antioxidants (11). Independently of their redox activity, Sesns lead to AMPK-dependent inhibition of TOR signaling and link genotoxic stress to TOR regulation (12). However, Sesns are also widely expressed in the absence of exogenous stress, and in *Drosophila*, expression of dSesn is increased upon maturation and aging (fig. S1C) (10). Given the redundancy between mammalian Sesns, we chose to test the importance of Sesns as regulators of TOR function in *Drosophila*. We generated both gain and loss of function *dSesn* mutants (fig. S2 to S4), whose analysis revealed that dSesn is an important negative feedback regulator of TOR whose loss results in various TOR-dependent, age-related pathologies.

Prolonged TOR signaling induces dSesn

Persistent TOR activation in wing discs by a constitutively active form of insulin receptor (InR^{CA}) resulted in prominent dSesn protein accumulation, not seen in a *dSesn*-null larvae (Fig. 1, A to C). InR^{CA} also induced accumulation of *dSesn* RNA (Fig. 1, D to F), indicating that dSesn accumulation is due to increased transcription or mRNA stabilization. As dSesn accumulation was restricted to cells in which TOR was activated, the response is likely to be cell autonomous. dSesn was also induced when TOR was chronically activated by overexpression of the small guanine triphosphatase Rheb (Fig. 1G), or clonal loss of PTEN (phosphatase and tensin homolog) or TSC1 (tuberous sclerosis complex 1) (Fig. 1, H and I). Dominant-negative PI3K ($PI3K^{DN}$) or TOR (TOR^{DN}) inhibited dSesn accumulation caused by overexpression of InR^{CA}, but inactive ribosomal S6 protein kinase (S6K; $S6K^{DN}$) and hyperactive 4E-BP ($4E\text{-}BP^{CA}$), two downstream TOR effectors, did not (fig. S5). Furthermore, dorsal-specific expression of activated $S6K^{CA}$ or loss of 4E-BP activity failed to induce dSesn expression (Fig. 1, J and K), indicating that TOR regulates expression of dSesn through different effector(s).

TOR signaling generates ROS to induce dSesn

In mammals, transcription of *Sesn* genes is increased in cells exposed to oxidative stress (9,11) and we observed ROS accumulation, detected by oxidation of dihydroethidium (DHE), in the same region of the imaginal discs in which InR^{CA} or Rheb were expressed (Fig. 2, A and B). InR^{CA}-induced accumulation of ROS was blocked by co-expression of either $PI3K^{DN}$ or TOR^{DN}, but not $S6K^{DN}$ or $4E\text{-}BP^{CA}$ (Fig. 2B), revealing TOR's role in ROS accumulation. Wing-disc clones in which TOR was activated by loss of TSC1 also exhibited ROS accumulation (Fig. 2C), confirming that TOR-dependent ROS accumulation is cell-autonomous. Expression of the ROS scavengers catalase or peroxiredoxin (13) inhibited InR^{CA}-induced accumulation of dSesn (Fig. 2, D and E). Feeding animals with vitamin E, an antioxidant, also prevented dSesn induction caused by TSC1 loss (Fig. 2F).

FoxO and p53 are ROS-activated transcription factors that control mammalian *Sesn* genes (9-12,14). The *dSesn* locus contains 8 perfect FoxO-response elements (fig. S6A), a frequency 25-times higher than that expected on the basis of random distribution.

Overexpressed FoxO or p53 could both increase expression of the *dSesn* gene (fig. S6, B to D). However, InR^{CA} caused accumulation of dSesn in a *p53*-null background (fig. S6E), but not in a *FoxO*-null background (fig. S6, F and J), indicating that TOR-activated FoxO (fig. S6, K to M) (15) is likely to be the regulator of *dSesn* gene transcription. Indeed, accumulation of dSesn in response to Rheb overexpression was also FoxO-dependent (fig. S6, G and H).

In dorsal wing disc cells, where ROS accumulated in response to InR^{CA} (Fig. 2A), JNK, a protein kinase that phosphorylates FoxO (13,14), was also activated (fig. S7, A and B). JNK activation was diminished in cells overexpressing catalase (fig. S7C), suggesting that it depends on TOR-induced accumulation of ROS. Mitogen-activated protein kinase kinase 7 (MKK7)-mediated activation of JNK also resulted in accumulation of dSesn (fig. S7, D and E), as did overexpression of Mst1 (mammalian STE20-like kinase 1), another protein kinase that phosphorylates FoxO (16), (fig. S7F). However, only JNK^{DN}, but not $Mst1^{DN}$, inhibited InR^{CA}-mediated accumulation of dSesn (fig. S7, G and H). Collectively, these data suggest that *dSesn* transcription is increased upon chronic TOR activation through ROS-dependent activation of JNK and FoxO (Fig. 2G).

dSesn antagonizes TOR-dependent cell and tissue growth

To determine effects of dSesn on cell growth, a major function of TOR (1-3), we overexpressed dSesn in dorsal wings (fig. S2F). This resulted in a dose-dependent phenotype in which the wing bends upwards (fig. S8, A to D), indicating suppressed dorsal tissue growth. A $dSesn^{C86S}$ variant, in which the cysteine required for oxidoreductase activity was mutated (11), still conferred this phenotype (fig. S8, E and F) when expressed in amounts similar to those of $dSesn^{WT}$ (fig. S3, A to D). We measured cell number and size in a dorsal wing region defined by the L3, L4, C1 and C2 veins (shaded in pink in fig. S8, G and H). Although the size of this area was significantly reduced by dSesn expression (fig. S8I), cell number remained unchanged (fig. S8J), showing that decreased cell size (fig. S8K) can account for dSesn suppression of tissue growth. Overexpression of dSesn also reduced cell size in larval wing discs (fig. S9) and adult eyes (fig. S10). Thus, dSesn inhibits cell growth without affecting cell proliferation independently of its redox activity.

When dSesn was expressed with InR^{CA} or Rheb, it suppressed the hyperplastic phenotypes caused by these TOR activators (Fig. 3, A to F). Both eye and individual ommatidia sizes were significantly reduced (Fig. 3G). dSesn also inhibited InR^{CA}- or Rheb-induced phosphorylation of TOR targets S6K and 4E-BP (Fig. 3H). In mammalian cells, dSesn enhanced AMPK-induced phosphorylation of TSC2 and inhibited S6K activity through TSC2 (fig. S11, A to C), just as mSesn2 does (12). In *Drosophila* wings, dSesn-induced growth suppression was attenuated by reduced gene dosage of TSC1, TSC2 or AMPK although reduced dosage of these genes alone did not affect normal growth (fig. S11, D and E). Expression of mSesn1/2 in flies (fig. S3, E and F) also reduced normal (fig. S12, A to C) and InR^{CA}-induced hyperplastic (fig. S12D) growth.

Expression of InR, constitutively active PI3K ($PI3K^{CA}$), AKT, or $S6K^{CA}$ in dorsal wing caused an overgrowth phenotype in which the wing bends downwards (Fig. 3, I and J; fig. S13, A to D). dSesn expression reversed this effect of overexpressed InR, $PI3K^{CA}$ and AKT, but not that of $S6K^{CA}$ (Fig. 3, K and L; fig. S13, E to H), suggesting that dSesn inhibits TOR downstream of AKT. Conversely, dorsal wing-specific expression of PTEN and dominant-negative InR (InR^{DN}), $PI3K^{DN}$, or $S6K^{DN}$ caused wings to bend upwards (fig. S13, I to L), and this effect was enhanced by dSesn (fig. S13, M to P).

Although *dSesn*-null flies did not exhibit developmental abnormalities, the growth promoting-effect of overexpressed InR or AKT was enhanced in *dSesn*-null background

(Fig. 3, M and N; fig. S14, A and B), suggesting that endogenous dSesn restricts TOR activation and its growth promoting effect. Loss of dSesn, however, did not enhance S6K-stimulated cell growth (fig. S14, C to F) or decrease growth suppression by overexpressed InR^{DN} or $S6K^{DN}$ (fig. S14, G to J). These findings indicate that Sesn is an evolutionarily conserved inhibitor of TOR signaling that acts via the AMPK-TSC2 axis (Fig. 3O).

dSesn reduces lipid accumulation

Fat bodies from *dSesn*-null third-instar larvae contained more lipids than did those of WT animals (Fig. 4A). *dSesn*-null adults also contained more triglycerides, which were decreased after ectopic expression of $dSesn^{WT}$ or $dSesn^{CS}$ (Fig. 4B; fig. S15). Thus, the TOR-inhibitory function of dSesn rather than its antioxidant activity appears to affect metabolic control. Congruently, *dSesn*-null fat bodies showed decreased AMPK and increased TOR activities (Fig. 4, C and D). Pharmacological manipulation strengthened this conclusion; feeding *dSesn*-null mutants with AMPK-activators such as AICAR (5-aminoimidazole-4-carboxamide 1-β-D-ribofuranoside) or metformin (4), or the TOR-inhibitor rapamycin (2) reduced triglyceride accumulation (Fig. 4B).

Expression of the gene encoding transcription factor dSREBP (5,17) and its targets, which encode fatty acyl CoA synthetase (dFAC), fatty acid synthase (dFAS), acetyl CoA carboxylase (dACC) and acetyl CoA synthetase (dACS) (17), was significantly increased (20-70%) in *dSesn*-null mutants (Fig. 4E). However, the PPAR-gamma coactivator 1 (dPGC-1) gene and some lipolytic genes showed decreased expression. This is consistent with reports that dSREBP and dPGC-1 are diametrically regulated by TOR and AMPK, respectively, to properly control lipid metabolism (1,2,4,5).

dSesn mutants exhibit a decline in cardiac performance

Age-related decline in heart performance is another phenotype associated with TOR hyperactivity in insects and mammals (18-20). In WT flies, the heart beats in a highly regular manner (Fig. 5A;movie S1), but in *dSesn*-null mutants heart function was compromised (Fig. 5B;movie S2) as manifested by arrhythmia (Fig. 5C) and decreased heart rate (Fig. 5D). Slowing of heart rate reflected expansion of the diastolic period (fig. S16A), as observed in aged or TOR-activated flies (18,21). These defects were largely prevented by feeding flies AICAR (Fig. 5E; movie S3) or rapamycin (Fig. 5F; movie S4), indicating they are caused by low activity of AMPK or high TOR activity. Vitamin E feeding or catalase expression suppressed the arrhythmia caused by loss of dSesn (Fig. 5, C and G) but not the decrease in heart rate (Fig. 5D), suggesting that TOR-induced oxidative stress contributes to the arrhythmic phenotype. Analysis of F-actin revealed structural disorganization of myofibrils in *dSesn*-null hearts (Fig. 5, H and I), suggesting that cardiac muscle degeneration may cause some of the functional defects in *dSesn*-null hearts. Reflecting this structural abnormality, *dSesn*-null hearts were dilated during both the diastolic and systolic phases, and this was prevented by AICAR or rapamycin (fig. S16B).

Heart-specific depletion of dSesn caused cardiac malfunction similar to that seen in *dSesn*-null mutants (fig. S17, A and B; movies S5 and S6). Heart-specific depletion of AMPK also caused cardiac malfunction, but this was not alleviated by AICAR administration (fig. S17, C to E; movie S7), supporting the notion that dSesn maintains normal heart physiology through AMPK activation.

Skeletal muscle degeneration and mitochondrial dysfunction caused by loss of dSesn

dSesn mRNA and protein are abundant in the adult thorax (fig. S18), which is mostly composed of skeletal muscle. mSesn1 is also highly expressed in skeletal muscle (10). We therefore tested whether dSesn has a role in maintaining muscle homeostasis. 20-day-old *dSesn*-null flies showed degeneration of thoracic muscles with loss of sarcomeric structure, including discontinued Z discs, disappearance of M bands, scrambled actomyosin arrays, and diffused sarcomere boundaries (Fig. 6, A and B;fig. S19, A to H). Such defects are only partially observed in very old WT flies (~90 days) (22), and were not found in young (5-day-old) *dSesn*-null muscles (fig. S19, I to L). Thus, the *dSesn*-null skeletal muscle appears to undergo accelerated aged-related degeneration.

Despite its normal appearance, muscle from 5-day-old *dSesn*-null flies exhibited mitochondrial abnormalities, including a rounded shape, occasional enlargement, and disorganization of cristae (fig. S19, I to L), which were also observed in 20-day-old mutants (fig. S19, E to H). Mitochondrial dysfunction can result in excessive generation of ROS leading to other abnormalities (23). Indeed, *dSesn*-null muscles exhibited increased accumulation of ROS, revealed by more intense DHE fluorescence and reduced *cis*-aconitase activity (fig. S20, A and B), which was associated with muscle cell death (fig. S20C). Furthermore, the muscle defects were prevented by vitamin E feeding (Fig. 6C), underscoring the role of ROS in muscle degeneration.

Expression of exogenous $dSesn^{CS}$, devoid of redox activity (11), prevented muscle degeneration (Fig. 6D), suggesting again that regulation of AMPK-TOR by dSesn, rather than intrinsic redox activity, is of importance. Indeed, feeding animals with AMPK activators prevented muscle degeneration in *dSesn*-null mutants (Fig. 6, E and F), and depletion of AMPK in skeletal muscles caused severe degeneration of mitochondrial and sarcomeric structures (Fig. S21, E to H). Treatment of animals with rapamycin also prevented muscle degeneration in *dSesn*-null flies (Fig. 6G). Thus, dSesn-dependent control of AMPK-TOR signaling is essential for prevention of mitochondrial dysfunction and maintenance of muscle homeostasis during aging.

Inhibition of autophagy phenocopies dSesn loss-of-function

We noticed that *dSesn*-null muscles accumulated polyubiquitin aggregates (fig. S20D), which are hallmarks of defective autophagy (24). To test whether decreased autophagy brought about by excessive and prolonged TOR activity (23) might cause muscle degeneration, we silenced expression of ATG1, an essential component of the autophagic machinery, which is inhibited by TOR (1, 6). This caused a decline in cardiac performance (Fig. 7, A to C; movie S8), and degeneration and mitochondrial abnormalities in skeletal muscle (Fig. 7D; fig. S21, I to L). These results suggest that TOR upregulation caused by dSesn loss inhibits autophagy needed to eliminate ROS-producing dysfunctional mitochondria (25), which may contribute to muscle degeneration. Consistent with this view, ATG1 silencing resulted in ROS accumulation in wing discs (Fig. 7E).

Discussion

The results described above identify *Sesn* as a feedback regulator of TOR function. In mammalian cells increased expression of mSesns in response to genotoxic stress leads to inhibition of TOR activity through activation of AMPK (12). We now show that transcription of the *dSesn* gene is increased upon chronic TOR activation through JNK and FoxO in a manner dependent on ROS accumulation. Although transient InR activation

inhibits FoxO through its phosphorylation by AKT (14), we find that chronic TOR activation overcomes this inhibition and results in nuclear translocation of FoxO, which increases *dSesn* transcription. In turn, dSesn suppresses metabolic dysfunction and age-related tissue degeneration brought about by hyperactivated TOR. Although dSesn can inhibit TOR-stimulated cell growth, our analysis points to its most important function being the maintenance of metabolic homeostasis and prevention of TOR-induced tissue degeneration. The three major functions of dSesn revealed by this study: suppression of lipid accumulation, prevention of cardiac malfunction and protection of muscle from age-related degeneration, are adversely affected by obesity, lack of exercise and aging, which make a disproportional contribution to health problems in developed and rapidly developing societies.

Whereas TOR controls cell growth mostly through inhibition of 4E-BP and activation of S6K kinase (1-3), its ability to induce dSesn expression depends on ROS accumulation, which our results suggest is a pathophysiological aberration caused by TOR hyperactivation that is normally antagonized by dSesn. However, the previously described redox function of Sesn (11) is not required for its protective role. TOR-induced accumulation of ROS was observed in yeast (26) and hematopoietic cells (27,28), but the molecular mechanism underlying this phenomenon and its physiological and pathophysiological significance were unknown. Our results suggest that TOR-stimulated accumulation of ROS, which is needed for accumulation of dSesn, is independent of two of the major TOR targets, 4E-BP and S6K, and instead may result from TOR-mediated inhibition of physiological autophagy, a process that eliminates ROS-producing dysfunctional mitochondria (23). Nonetheless, inhibition of 4E-BP also contributes to the pro-aging effects of TOR by suppressing translation of several mitochondrial proteins (29) and by accelerating age-related cardiac malfunction at young ages (20), which is reminiscent of the observed cardiac defects seen in *dSesn*-null flies. Although TOR activates SREBP (17) and this may contribute to lipid accumulation in *dSesn*-null flies, autophagy promotes lipid elimination (30). Thus, decreased autophagy may also contribute to triglyceride accumulation. Hence, the different degenerative phenotypes exhibited by *dSesn*-null flies are due to the cumulative effects of several biochemical and cell biological defects caused by hyperactive TOR, including reduced autophagy and reduced function of 4E-BP. Both basal physiologic autophagy and 4E-BP function are enhanced by CR, which prevents aging-related pathologies (31). In the future, it will be of interest to determine the contribution of Sesn to these anti-aging effects.

Supplementary Material

Refer to Web version on PubMed Central for supplementary material.

Acknowledgments

We thank W. Mcginnis (UCSD), M. Tatar (Brown Univ.), S. Oldham (Burnham Institute), U. Banerjee (UCLA), I.K. Hariharan (UC Berkeley), J. Brenman (UNC), O. Puig (Merck), C. Wilson (Oxford Univ.), L. Jones (Salk Institute), M. Miura (Univ. of Tokyo), DSHB (Iowa), DGRC (Indiana), DGRC (Japan), VDRC (Austria), Cell Signaling Inc., Santa Cruz Biotech. Inc., Bloomington and Harvard stock centers for fly strains, reagents and access to lab equipment. We acknowledge help from J. Kim, M. Yoon and R. Anderson in EM analysis, V. Temkin in ROS analysis, and M. Smelkinson, O. Cook and A. Guichard in histochemistry. We thank M. Kim for suggestions and constructive criticism. Work was supported by grants and fellowships from the NIH and Superfund Research Program (CA118165, ES006376 and P42-ES010337 to M.K., DK082080 to A.B., P41-RR004050 and P30-CA23100 to M.H.E.), KRF (KRF-2007-357-C00096 to J.H.L.), HFSPO (LT00653/2008-L to J.H.L), and NSERC (to E.J.P.). M.K. is an American Cancer Society Professor.

References and Notes

1. Wullschleger S, Loewith R, Hall MN. Cell 2006;124:471. [PubMed: 16469695]

2. Hay N, Sonenberg N. Genes Dev 2004;18:1926. [PubMed: 15314020]
3. Oldham S, Hafen E. Trends Cell Biol 2003;13:79. [PubMed: 12559758]
4. Towler MC, Hardie DG. Circ Res 2007;100:328. [PubMed: 17307971]
5. Porstmann T, et al. Cell Metab 2008;8:224. [PubMed: 18762023]
6. Chan EY. Sci Signal 2009;2:pe51. [PubMed: 19690328]
7. Harrison DE, et al. Nature 2009;460:392. [PubMed: 19587680]
8. Kapahi P, Zid B. Sci Aging Knowledge Environ 2004;2004:PE34. [PubMed: 15356349]
9. Budanov AV, et al. Oncogene 2002;21:6017. [PubMed: 12203114]
10. Velasco-Miguel S, et al. Oncogene 1999;18:127. [PubMed: 9926927]
11. Budanov AV, Sablina AA, Feinstein E, Koonin EV, Chumakov PM. Science 2004;304:596. [PubMed: 15105503]
12. Budanov AV, Karin M. Cell 2008;134:451. [PubMed: 18692468]
13. Owusu-Ansah E, Yavari A, Mandal S, Banerjee U. Nat Genet 2008;40:356. [PubMed: 18246068]
14. Greer EL, Brunet A. Oncogene 2005;24:7410. [PubMed: 16288288]
15. Harvey KF, et al. J Cell Biol 2008;180:691. [PubMed: 18299344]
16. Lehtinen MK, et al. Cell 2006;125:987. [PubMed: 16751106]
17. Dobrosotskaya IY, Seegmiller AC, Brown MS, Goldstein JL, Rawson RB. Science 2002;296:879. [PubMed: 11988566]
18. Wessells RJ, Fitzgerald E, Cypser JR, Tatar M, Bodmer R. Nat Genet 2004;36:1275. [PubMed: 15565107]
19. Luong N, et al. Cell Metab 2006;4:133. [PubMed: 16890541]
20. Wessells R, et al. Aging Cell 2009;8:542. [PubMed: 19594484]
21. Ocorr K, et al. Proc Natl Acad Sci U S A 2007;104:3943. [PubMed: 17360457]
22. Takahashi A, Philpott DE, Miquel J. J Gerontol 1970;25:222. [PubMed: 5454408]
23. Yen WL, Klionsky DJ. Physiology (Bethesda) 2008;23:248. [PubMed: 18927201]
24. Hara T, et al. Nature 2006;441:885. [PubMed: 16625204]
25. Zhang Y, et al. Autophagy 2007;3:337. [PubMed: 17404498]
26. Bonawitz ND, Chatenay-Lapointe M, Pan Y, Shadel GS. Cell Metab 2007;5:265. [PubMed: 17403371]
27. Chen C, et al. J Exp Med 2008;205:2397. [PubMed: 18809716]
28. Kim JH, et al. Blood 2005;105:1717. [PubMed: 15486067]
29. Zid BM, et al. Cell 2009;139:149. [PubMed: 19804760]
30. Singh R, et al. Nature 2009;458:1131. [PubMed: 19339967]
31. Colman RJ, et al. Science 2009;325:201. [PubMed: 19590001]

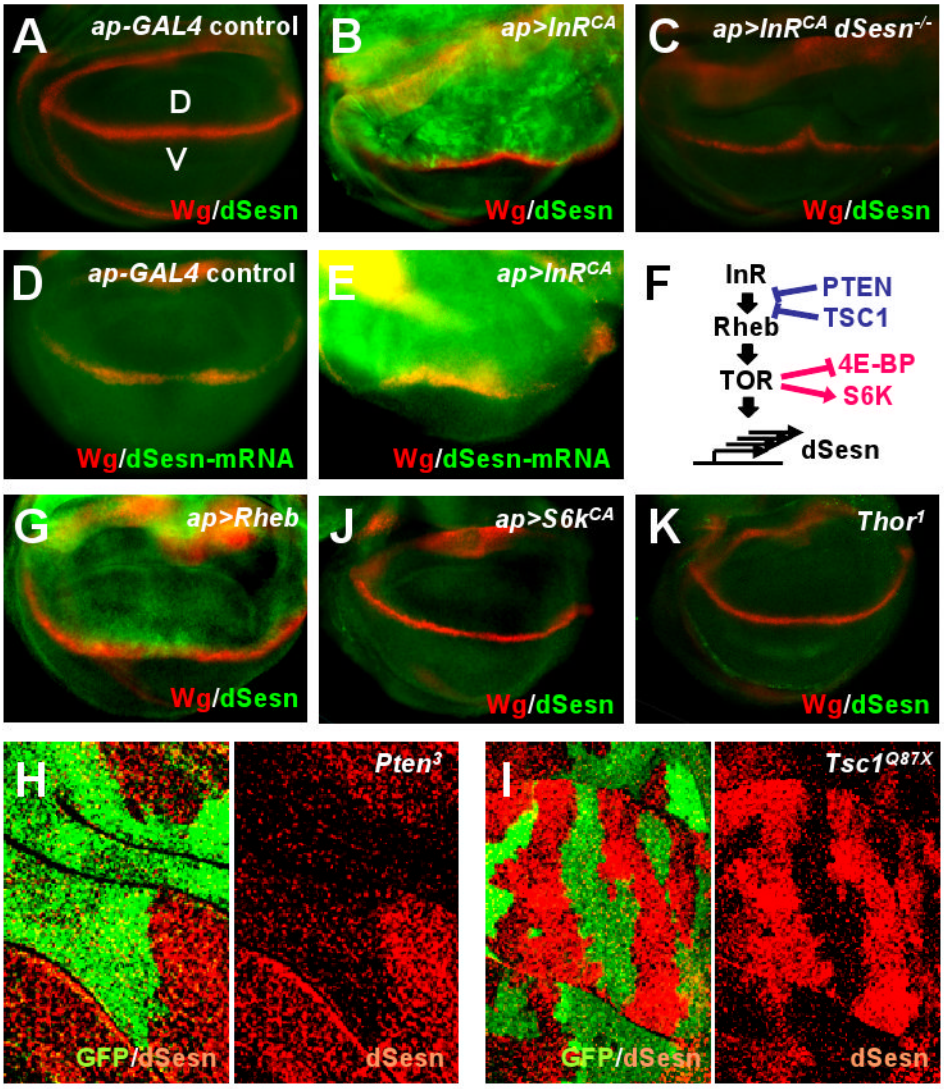

Fig. 1.

Increased abundance of dSesn upon TOR activation. Larval wing discs of indicated strains were stained to visualize indicated proteins or mRNA. The dorsal side points upwards. Dorsoventral boundary (D/V in A) was visualized by staining with an antibody to the wingless (Wg) protein (red). (**A** to **C**) Expression of dSesn protein (green) in the absence (A) or presence of InR^{CA} in WT (B) and *dSesn*-null (C) strains. (**D** and **E**) Accumulation of dSesn mRNA (green) in response to InR^{CA} detected by in situ hybridization. (**F**) The signaling network controlling TOR activity and expression of dSesn. (**G** to **K**) Accumulation of dSesn (green) in response to Rheb (G) but not $S6K^{CA}$ (J) or loss of 4E-BP (K). *Thor*^{1} is a *Drosophila* 4E-BP loss-of-function mutant. (**H** and **I**) Accumulation of dSesn after somatic loss of PTEN (H) or TSC1 (I). Absence of GFP (green) indicates loss of PTEN or TSC1 resulting in dSesn (red) accumulation.

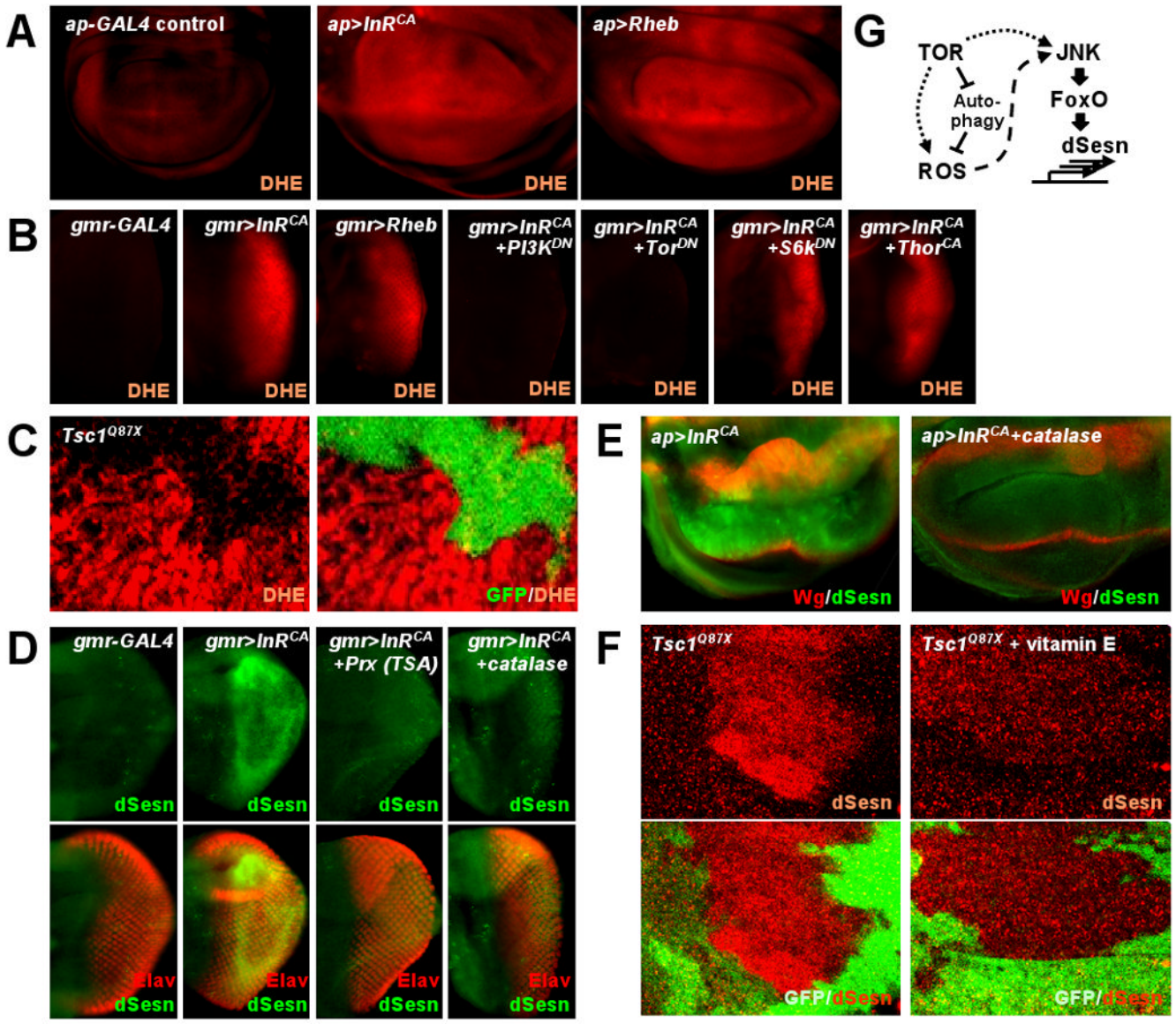

Fig. 2.

Chronic TOR activation results in accumulation of ROS and dSesn. Larval imaginal discs of indicated strains were stained as indicated. (**A**) ROS accumulation (red) in response to InR^{CA} or Rheb overexpressed in dorsal (upwards) wing discs was revealed by DHE staining. (**B**) InR^{CA}-induced ROS (red) accumulation in eye discs was reduced by $PI3K^{DN}$ or TOR^{DN} but not by $S6K^{DN}$ or 4E-BP^{CA}. (**C**) DHE staining (red) in TSC1-negative wing disc clones marked by absence of GFP. (**D** and **E**) Inhibition of InR^{CA}-induced accumulation of dSesn (green) in eye and wing discs by expression of catalase or peroxiredoxin (Prx). D-V wing boundary and differentiated eye area were visualized by Wg (red) and Elav (red) staining, respectively. (**F**) dSesn accumulation (red) in TSC1-negative wing disc clones was suppressed by vitamin E feeding. Absence of GFP (green) indicates loss of TSC1. (**G**) Diagram depicting TOR-stimulated production of ROS and expression of dSesn.

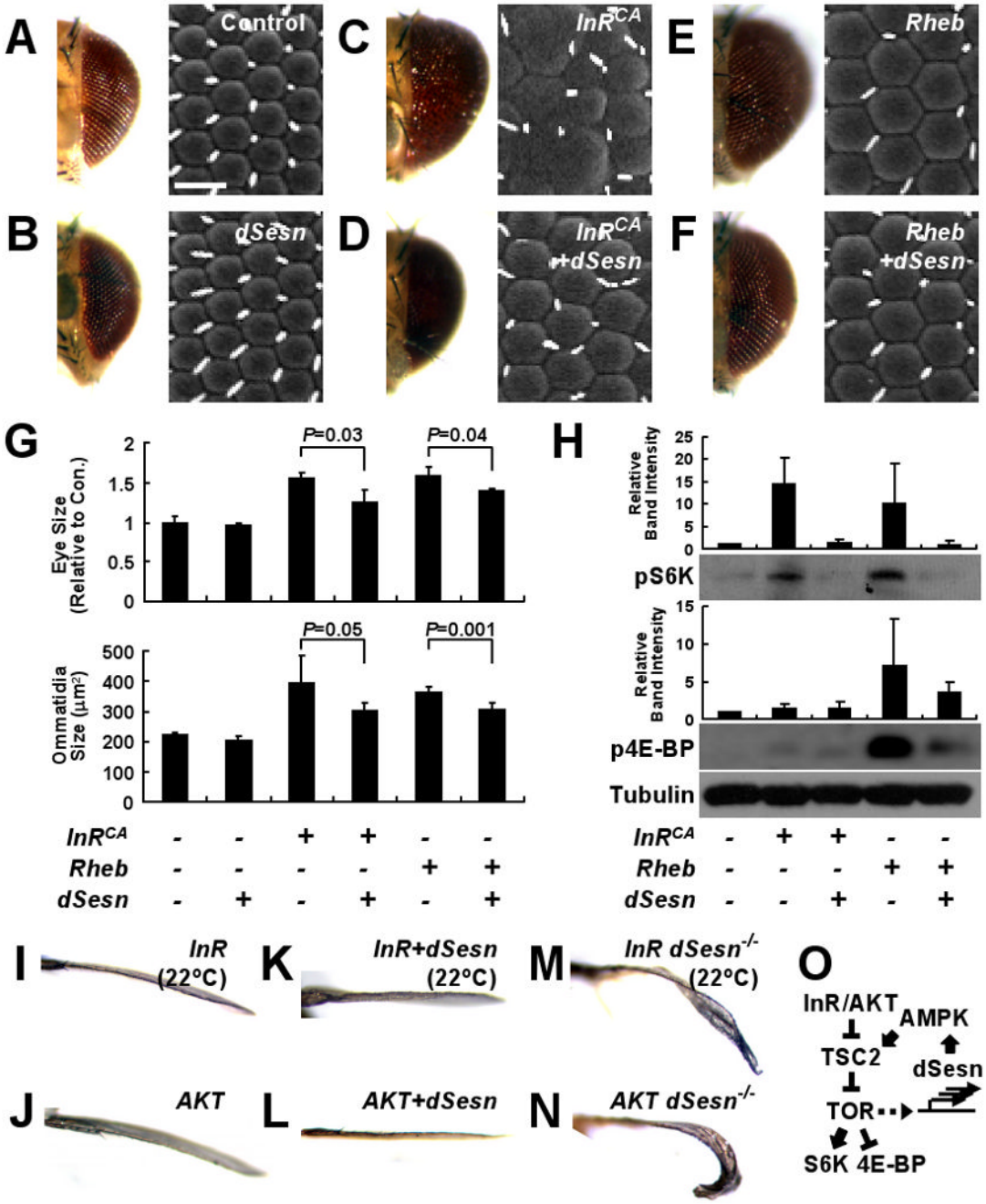

Fig. 3.

Antagonism of TOR-stimulated growth by dSesn. (**A** to **F**) Light (left) and scanning electron (right) micrographs of eyes expressing the indicated genetic elements driven by *gmr-GAL4*. Scale bar, 20 μm. (**G**) Quantification of eye and ommatidia sizes measured from frontal and lateral views, respectively. *P* values were calculated by one-way ANOVA. Error bars=S.D.; n=3 and 5, respectively. (**H**) Suppression of TOR signaling by dSesn. Adult heads with eye-specific expression of indicated genetic elements driven by *gmr-GAL4* were subjected to immunoblot analyses with indicated antibodies. Relative band intensities were quantified and are presented as bar graphs. Error bars=S.D. n=3. (**I** to **N**) Suppression of InR-induced growth by dSesn. Anterior views of wing blades with *apterous-GAL4*-driven expression of

indicated genetic elements. Dorsal sides point upwards. (**O**) Schematic diagram summarizing genetic interactions between dSesn and TOR signaling components.

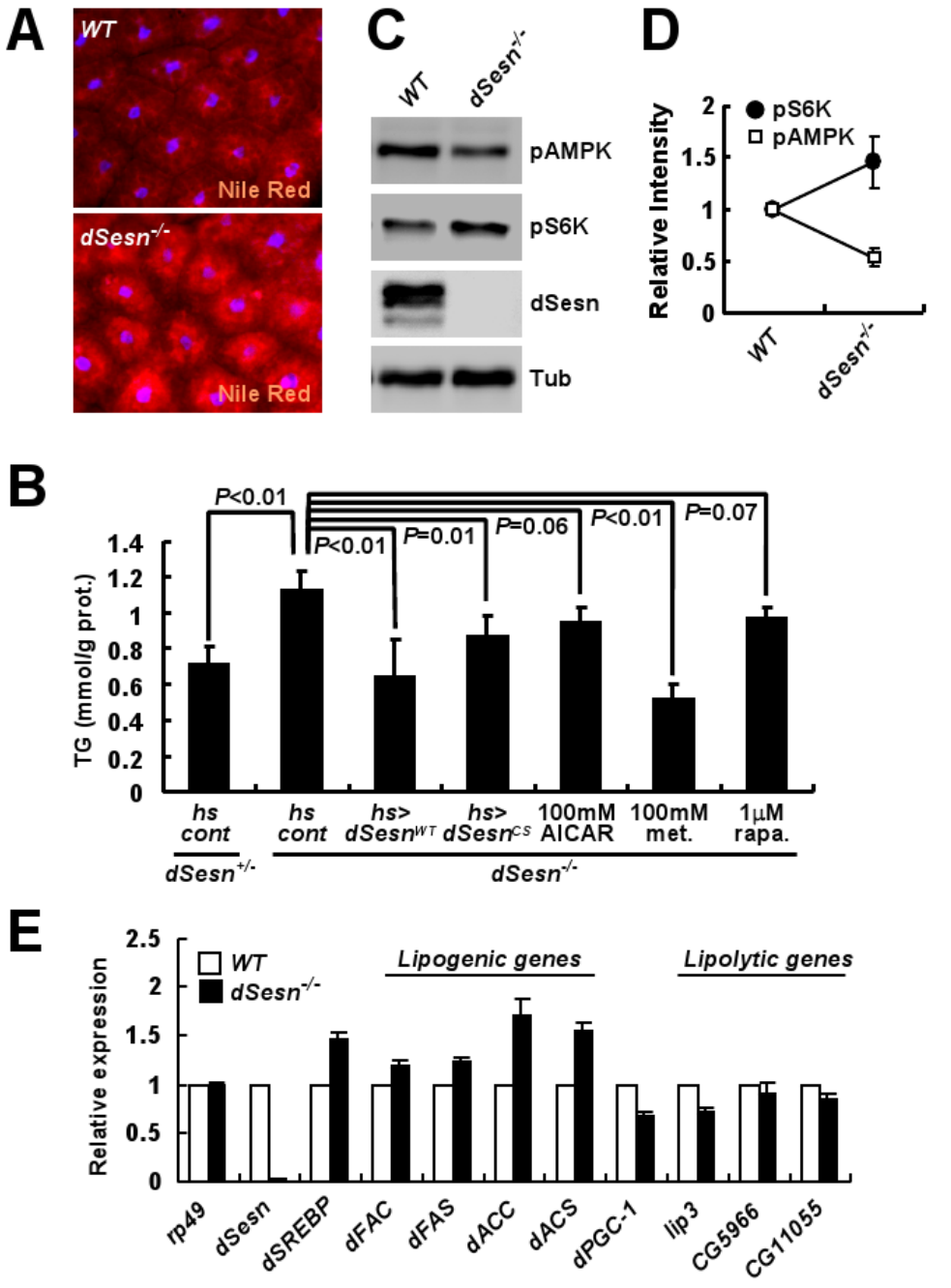

Fig. 4.

Effect of dSesn on lipid homeostasis. (**A**) Lipid accumulation in fat bodies examined by Nile Red staining (red). (**B**) Total triglycerides were measured in five 10-day-old adult males of the indicated genotypes subjected to the indicated treatments (met., metformin; rapa., rapamycin). *P* values were calculated by one-way ANOVA. Error bars=S.D.; n≥3. (**C** and **D**) Protein lysates from fat bodies were analyzed by immunoblotting with indicated antibodies. Relative band intensities were quantified and are shown as a bar graph. Error bars=S.D.; n=3. (**E**) Expression of indicated mRNAs in adult flies was examined by quantitative RT-PCR. Fifty 3-day-old adult males of each genotype were used to prepare total RNA. Error bars=S.D.; n=3.

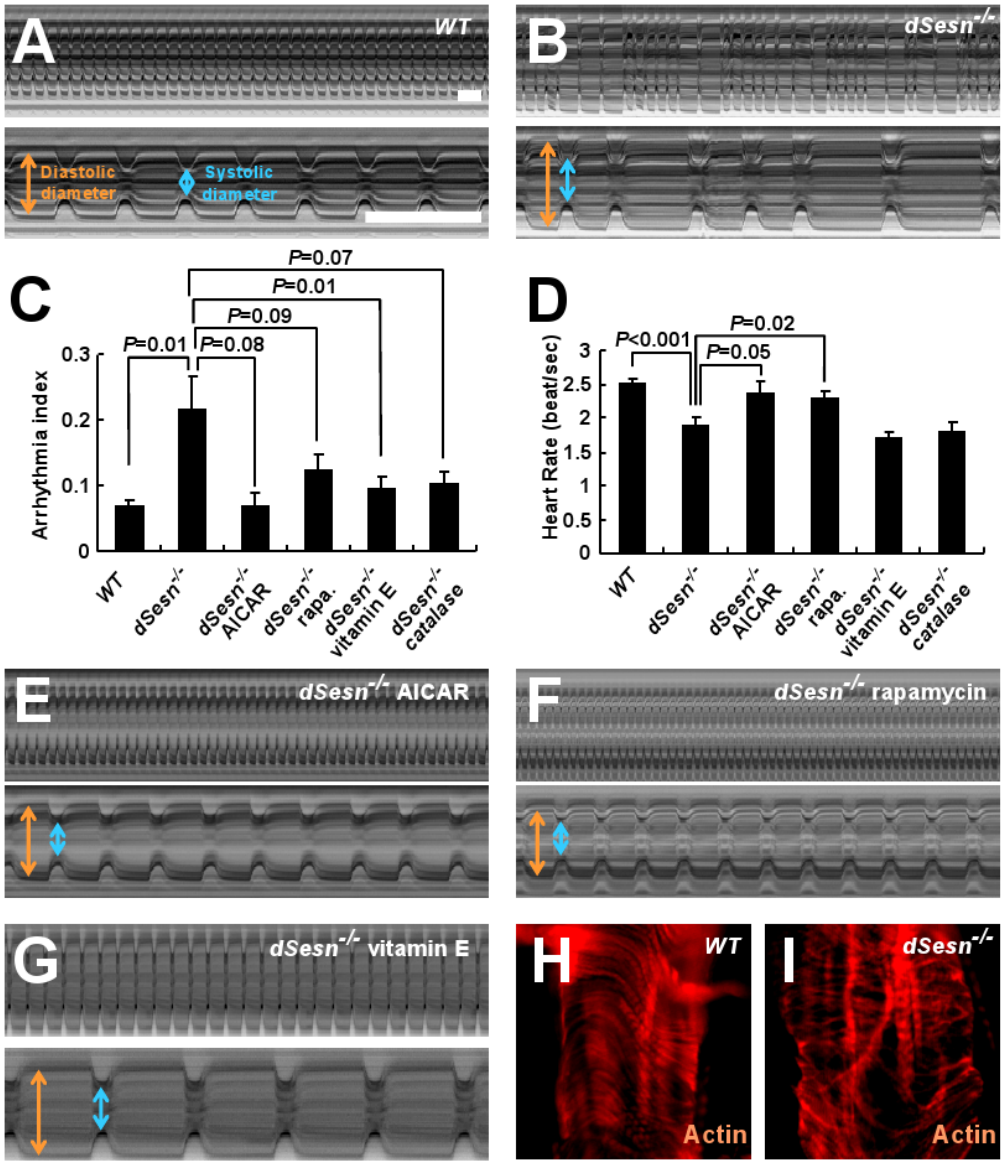

Fig. 5.

Effect of dSesn on cardiac function. (**A, B, E** to **G**) Representative M mode records of indicated 2-week-old flies fed without or with indicated drugs, showing movement of heart tube walls (y-axis) over time (x-axis). Diastolic (orange) and systolic (blue) diameters are indicated. 1 second is indicated as a bar. (**C** and **D**) Quantification of cardiac function parameters. *P* values were calculated using one-way ANOVA. Error bars indicate S.E.M.; n>10. (**H** and **I**) Actin fibers in WT and *dSesn*-null hearts were visualized by phalloidin staining (red).

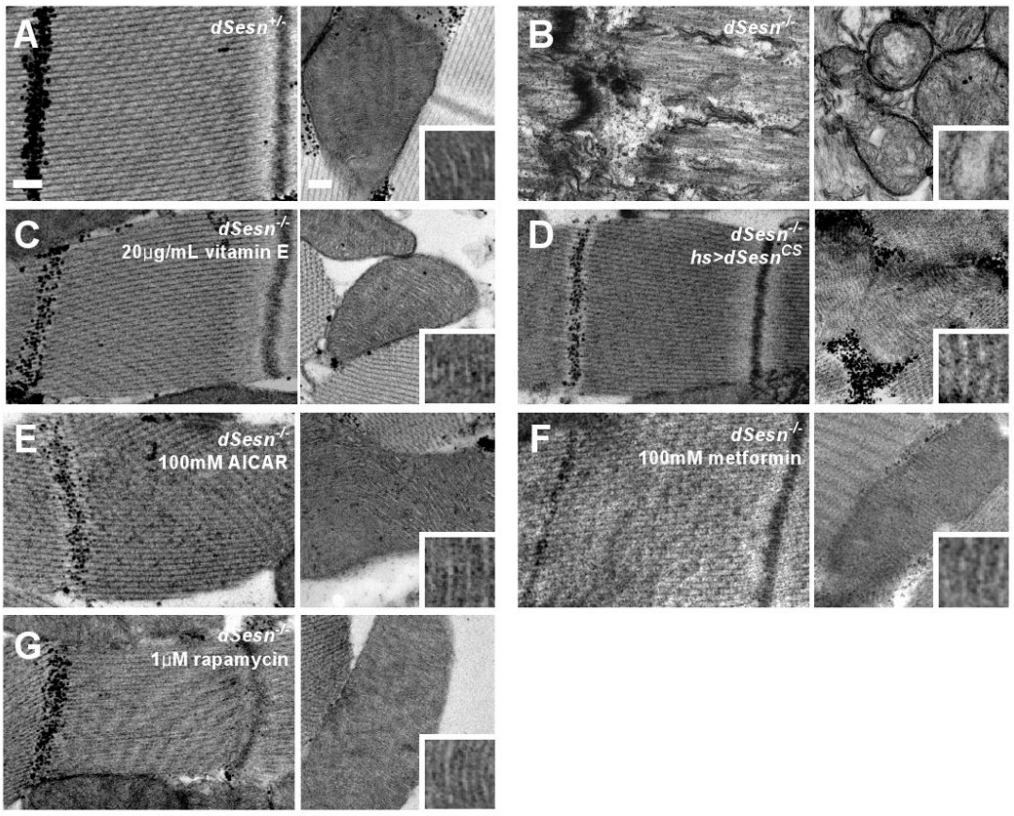

Fig. 6.

Effect of dSesn on progressive muscle degeneration. Thoracic skeletal muscles of indicated 20-day-old male flies treated without or with indicated drugs were analyzed by transmission electron microscopy (TEM). Left panels: sarcomeres; right panels: mitochondria. Mitochondrial microstructure is shown in the insets (0.15 μm width). Scale bars, 0.2 μm.

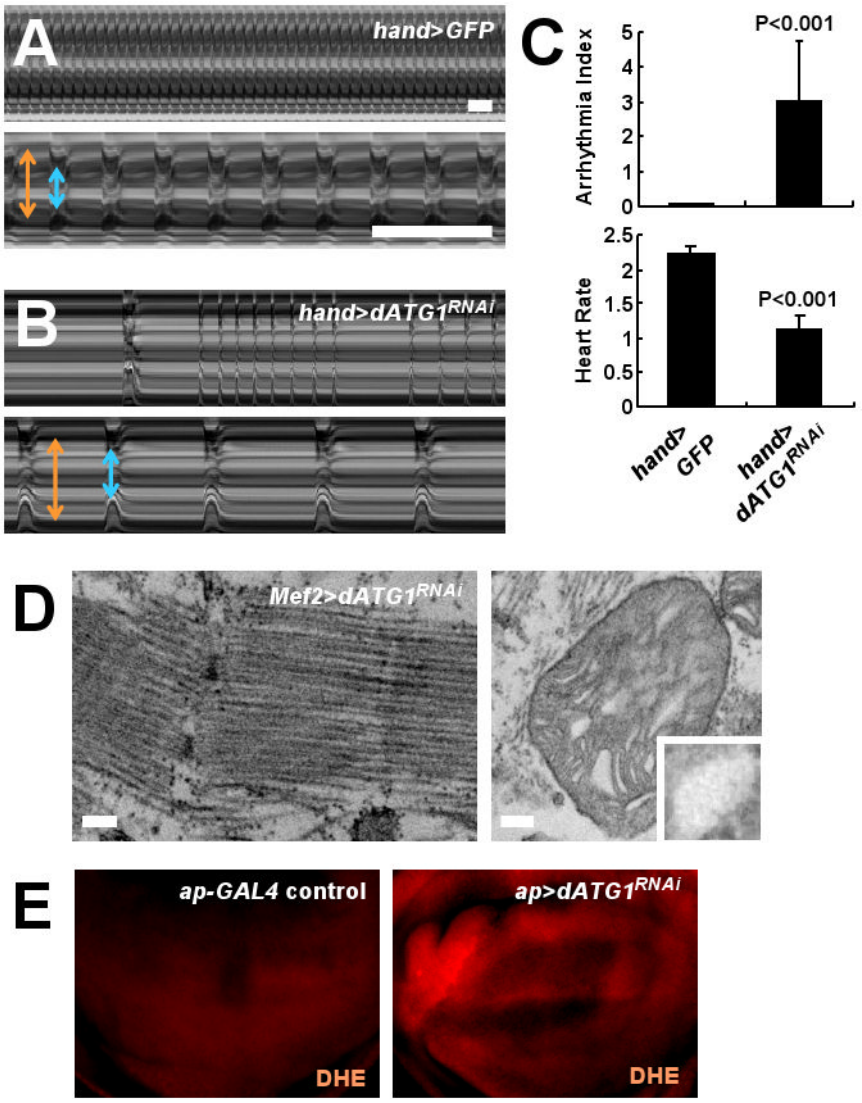

Fig. 7.

Phenotypes caused by silencing of dATG1. (**A** and **B**) Representative M mode records of control and *dATG1*^{RNAi}-expressing hearts from 2-week-old adult flies, showing the movement of heart tube walls (y-axis) over time (x-axis). Diastolic (orange) and systolic (blue) diameters are indicated. 1 second is indicated as a bar. (**C**) Quantification of cardiac function parameters. *P* values were calculated using one-way ANOVA. Error bars indicate S.E.M.; n≥9. (**D**) *dATG1*^{RNAi}-expressing thoracic skeletal muscle was analyzed by TEM. Left panel: sarcomeres; right panel: mitochondria. Mitochondrial microstructure is shown in the insets (0.15 μm width). Scale bars, 0.2 μm. (**E**) ROS accumulation (red) in response to *dATG1*^{RNAi} expressed in dorsal (upwards) wing discs revealed by DHE staining.